FLOW OF CONCENTRATED POLYMER SOLUTIONS IN MODEL CHANNELS

G. A. Belinskii, T. M. Getmanyuk, V. G. Kulichikhin, and A. L. Yarin

UDC 532.135

Measurements are made of the distribution of longitudinal stresses in the flow of polymer systems in plane channels. The coefficients of expansion of free jets leaving cylindrical channels are also measured. The experimental data is compared with calculated results.

The study of flows of concentrated polymer systems in the channels of spinnerettes is important from the viewpoint of intensifying the formation of chemical fibers [1]. It is also of considerable practical interest to investigate the expansion of jets of polymer liquids at the outlet of such channels and to predict the degree of expansion.

We conducted an experimental study of the flow of concentrated polymer solutions in plane-slit channels with different configurations of the inlet region. The channels modeled the channels in spinnerettes (the latter have cross sections in the form of a circle). Experimental data on the stress distribution along the model plane channels was obtained by the photoelastic method [2]. The tests were conducted on a unit which made it possible to record the interference fringes of isochromatic lines (lines representing identical differences in the principal stresses) and isoclinic lines (lines representing identical directions of the planes of polarization of the incident light and the principal stresses) in the flow of spinning solutions through channels of plane cross section with transparent walls. The unit (Fig. 1) includes an isobaric capillary-type gas viscometer and an optical system. The characteristics of the channels we used are shown in Table 1 (also see Fig. 2a and d).

The object of our study was a 4% solution of polyamidebenzimidazole (PABI) in dimethylacetamide. The solution had a viscosity at zero shear rate η_0 = 31 Pa·sec and a molecular weight $\bar{M}_W \sim 50{,}000$. The latter was evaluated by the method used in [3]. We used a PIRSP-1m flow goniometer to obtain the dependences of the shear stress τ_{xy} and the first difference of the normal stresses N_1 on the shear rate $\dot{\gamma}$ for the investigated PABI solutions. The shear rate varied within the range from 10^{-3} to 10 sec^{-1}. We then used these dependences extrapolate to the zero value of $\dot{\gamma}$ and calculate the high-elasticity coefficient $G = (2\tau_{xy}^2/N_1)|_{\dot{\gamma}\to 0}$. This coefficient turned out to have a value of 2100 Pa.

It follows from the relations of the photoelastic method [2] that

$$\tau_{xx} - \tau_{yy} = \frac{n\lambda}{Cd}\cos 2\varkappa. \qquad (1)$$

The dynamic optical coefficient C, determined in accordance with the method in [4], was $2.2\cdot10^{-7}$ Pa^{-1}. This is nearly two orders greater than the values of C obtained for flexible-chain elastomer-polybutadienes and polyisoprenes [5]. The values of n and $\varkappa$ are determined experimentally from the interference patterns of the flow of a PABI solution.

The $\tau_{xx} - \tau_{yy}$ stresses in the experiment can be calculated only near the channel inlet (at a certain distance from the edges of the inlet) due to the rapid relaxation of the quantity $\tau_{xx} - \tau_{yy}$ to zero as we consider points deeper in the channel – farther from the section where the contraction ceases (x = 0). It should be noted that in contrast to the present study, in [1] it was found to be expedient to assume that x = 0 at the channel outlet.

Figure 2 shows the distribution of the stresses $\tau_{xx} - \tau_{yy}$ along the axis of channels 1-4 for different flow rates. It is evident that the stresses rapidly increase as the chan-

Institute of Problems of Mechanics, Academy of Sciences of the USSR, Moscow. "Khimvolokno" Scientific-Industrial Association, Moscow. Translated from Inzhernerno-Fizicheskii Zhurnal, Vol. 55, No. 1, pp. 59-66, July, 1988. Original article submitted February 9, 1987.

0022-0841/88/5501-0745 $12.50

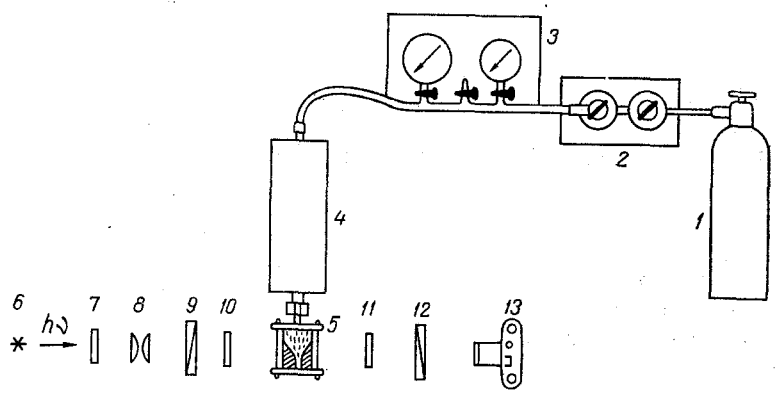

Fig. 1. Diagram of the experimental unit: 1) high-pressure gas cylinder; 2) regulator control panel; 3) monitoring-measuring instrument panel; 4) viscometric tank; 5) optical cell; 6) source of monochromatic radiation with a wavelength λ = 546 nm; 7) light filter; 8) condenser; 9) polarizer; 10, 11) four-wave plates; 12) analyzer; 13) photographic recorder.

TABLE 1. Characteristics of the Plane-Slit Channels

Number of channel	2α	$l\cdot10^3$	$L_1\cdot10^3$	$D_-\cdot10^3$	$D_0\cdot10^3$	$W\cdot10^3$
	m					
1	30°	30,0	16,8	1	10	6,1
2	45°	28,6	10,9	1	10	6,1
3	90°	30,0	4,5	1	10	6,1
4	Curving $r=5\cdot10^{-3}$m	40,0	5	1	10	6,1

nel is constricted, reaching a maximum near the section where the constriction ends. The stresses then quickly relax.

Let us proceed to description of the experimental study of expansion of free jets leaving channels of model spinnerettes (Barris effect). In the present case, along with a PABI solution we used a 5% solution of poly-p-phenylene-1,3,4-oxadiazole (POD) in concentrated sulfuric acid with flow through calibrated holes which modeled spinnerette channels. The POD solution had a viscosity at zero shear rate η_0 = 230 Pa·sec. The molecular weight of the polymer $\bar{M}_W$ ~ 48,000 (according to [6]). Using the method described above for the PABI solution in experiments on a PIRSP-1m goniometer, we determined the high-elasticity modulus G of the POD solution. It turned out to be equal to 700 Pa. The geometric parameters of the calibrated holes which modeled the spinnerette channels are shown in Table 2 (a diagram of these holes is shown in Fig. 2a).

The studies were conducted on the unit described above (see Fig. 1) in the pressure interval ΔP = 10-500 KPa and flow-rate interval $q = (0.01\text{-}3.6)\cdot10^{-7}$ m^3/sec. In the experiments, the shear rate on the walls of the channels changed within the range $\dot{\gamma} = 10^2\text{-}6\cdot10^3$ sec^{-1}. The jet of PABI or POD solution leaving the channel was photographed under an MBS-2 microscope with a magnification of 30. The results were then subjected to photometric analysis.

The dependences of the coefficient of expansion of the jet $B_* = D_+/D_-$ on flow rate q are shown in Figs. 3 and 4 by points (for the PABI and POD solutions, respectively). It is evident that B_* increases monotonically with an increase in q.

Let us theoretically analyze the flows studied in the experiments. As was shown in [7], within a fairly broad range of strain rates up to very high values (specifically, ~10^3 sec^{-1}), the rheological behavior of concentrated polymer systems is described by the relation

$$\frac{d\tau}{dt} = \nabla v\cdot\tau + \tau\cdot\nabla v^T + \frac{2}{3}G_0\mathbf{D} - \frac{1}{\tau_B}(\tau-\tau_2) - \frac{\tau}{\tau_C}. \quad (2)$$

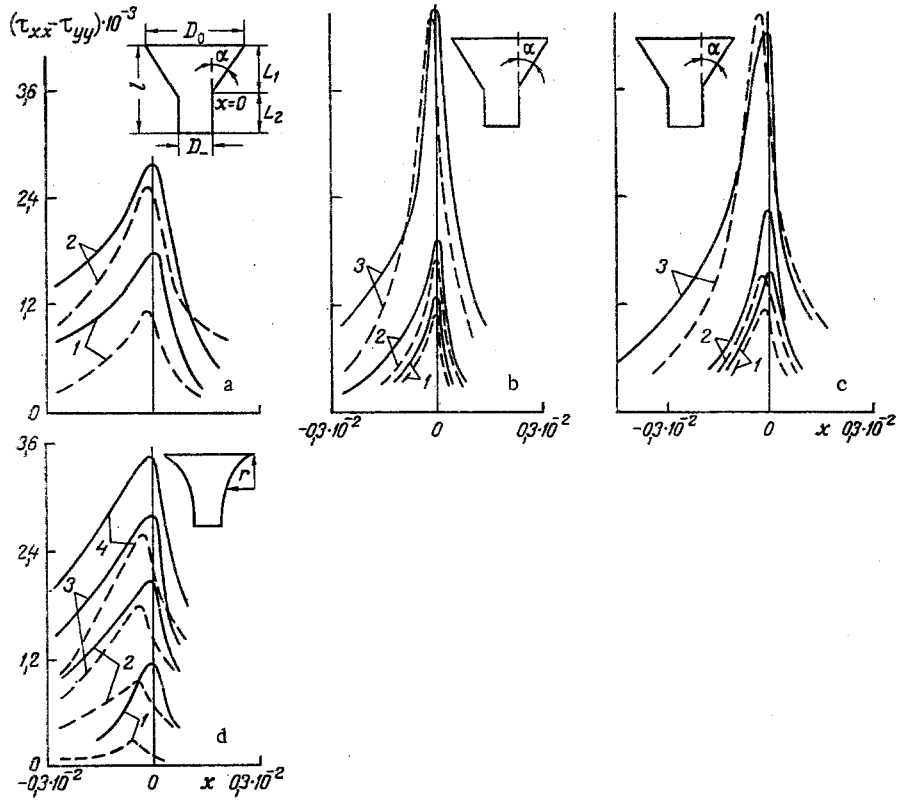

Fig. 2. Distribution of the first difference of the normal stresses along the axis with flow in model plane-slit channels (solid curves show results of calculations, dashed curves show experimental data): a) channel 1 (see Table 1): 1) q = $0.176\cdot10^{-6}$ m^3/sec; 2) $0.462\cdot10^{-6}$; b) channel 2: 1) q = $0.105\cdot10^{-6}$ m^3/sec; 2) $0.158\cdot10^{-6}$; 3) $0.605\cdot10^{-6}$; c) channel 3: 1) q = $0.059\cdot10^{-6}$ m^3/sec; 2) $0.094\cdot10^{-6}$; 3) $0.34\cdot10^{-6}$; d) channel 4: 1) q = $0.055\cdot10^{-6}$ m^3/sec; 2) $0.157\cdot10^{-6}$; 3) $0.269\cdot10^{-6}$; 4) $0.433\cdot10^{-6}$. $\tau_{xx}-\tau_{yy}$, N/m^2; x, m.

TABLE 2. Geometric Parameters of Calibrated Holes Modeling Spinnerette Channels

2α	$l\cdot10^3$	$L_1\cdot10^3$	$L_2\cdot10^3$	$D_-\cdot10^3$
	m			
20°	0,812	0,406	0,406	0,406
31°30′	0,812	0,406	0,406	0,406
45°30′	0,812	0,406	0,406	0,406
60°	0,812	0,406	0,406	0,406
91°	0,812	0,406	0,406	0,406
120°	0,812	0,406	0,406	0,406

If the characteristic hydrodynamic time t_0 is on the order of the relaxation time τ_C or exceeds it and if the strain rates are low ($\sim\tau_C^{-1}$), then Eq. (2) is simplified. If we ignore the higher orders ($\tau_C \gg \tau_B$), this equation reduces to the equality $\tau = \tau_2$ [7]. Here, in contrast to [1, 7], we will use a multimodal expression for the stresses τ_2 due to disequilibrium of the system of bonding points of the macromolecule (this does not change the character of the problem and has almost no effect on the quantitative charactristics). Thus, in the above-indicated limiting case, Eq. (2) reduces to the multimodal Doi–Edwards rheological governing equation (RGE)

$$\boldsymbol{\tau} = \boldsymbol{\tau}_2 = G_0 \sum_{j_{\text{odd}}=1}^{\infty} \frac{8}{\pi^2\tau_1} \int_{-\infty}^{t} d\tau \exp\left[-\frac{(t-\tau)\,j^2}{\tau_1}\right]\left[\mathbf{Q}(t,\ \tau) - \frac{\mathbf{I}}{3}\right], \tag{3}$$

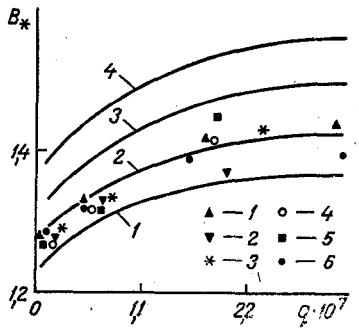

Fig. 3

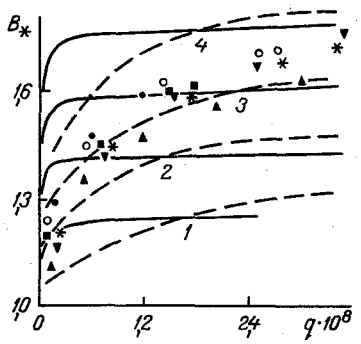

Fig. 4

Fig. 3. Dependence of the coefficient of expansion of the jet B_* on the rate of flow of the PABI solution with different values for the inlet angle of the spinnerette channel α: experimental points: 1) $2\alpha = 20°$; 2) 31°31'; 3) 45°30'; 4) 60°; 5) 91°; 6) 120°; theoretical curves: 1) $2\alpha = 20°$; 2) 25°; 3) 31°30'; 4) 35°30'. q, m^3/sec.

Fig. 4. Dependence of the coefficient of expansion of the jet B_* on the rate of flow of the POD solution with different values for the inlet angle of the spinnerette channel α: experimental points 1-6, see Fig. 3; theoretical curves: 1) $2\alpha = 20°$; 2) 30; 3) 40; 4) 50° (solid curves – $\tau_B = 0.3$ sec; dashed curves – 0.03 sec).

$$\mathbf{Q} = \int \frac{d^2\mathbf{u}_0}{4\pi} \left\{ \frac{[\mathbf{F}_\tau(t)\cdot\mathbf{u}_0]\,[\mathbf{F}_\tau(t)\cdot\mathbf{u}_0]}{|\mathbf{F}_\tau(t)\cdot\mathbf{u}_0|^2} \right\}, \quad \eta_0 = \frac{\pi^2}{60} G_0\tau_1, \quad G_0 = 6G.$$

Using the values of η_0 and G obtained for the PABI solution in the shear experiments to calculate the modulus G_0 and relaxation time τ_1, in accordance with the last two equations of (3) we have G_0 = 12,600 Pa and τ_1 = 0.015 sec. The characteristic time of flow of the solution in the investigated plane channels (the residence time in the constricted part of the channel) $t_0 \sim 0.1$ sec $> \tau_1$, while the strain rate $\sim 10\text{-}10^2$ sec$^{-1} \sim \tau_1^{-1}$. Thus, in accordance with [7], the use of the RGE to calculate flows in model plane channels is fully valid, since the dominant mechanism of relaxation at $t_0 > \tau_1$ and strain rates on the order of τ_1^{-1} is diffusion of macromolecules.

Having in mind anomaly of viscosity – typical of viscoelastic spinning solutions – which reduces friction against the wall, we will assume that the flow of a polymer solution in a convergent channel can be approximately represented as a quasiunidimensional flow under uniaxial tension [1]. Thus, in the case of a plane channel, we use (3) to find the following expressions for the components of the tensor Q:

$$Q_{xx} = \lambda_1^2 \int_0^1 dm \frac{m^2}{\sqrt{m^4(\lambda_1^4 - 1 - \lambda_1^2 + \lambda_1^{-2}) + m^2(1 + \lambda_1^2 - 2\lambda_1^{-2}) + \lambda_1^{-2}}},$$

$$Q_{yy} = \frac{\lambda_1^{-2}}{1 - \lambda_1^{-2}} \int_0^1 dm \left[\sqrt{\frac{\lambda_1^2 m^2 + 1 - m^2}{\lambda_1^{-2} - \lambda_1^{-2} m^2 + \lambda_1^2 m^2}} - 1 \right], \tag{4}$$

$$Q_{zz} = \frac{1}{1 - \lambda_1^{-2}} - \frac{1}{1 - \lambda_1^{-2}} \int_0^1 dm \sqrt{\frac{(\lambda_1^2 - \lambda_1^{-2}) m^2 + \lambda_1^{-2}}{(\lambda_1^2 - 1) m^2 + 1}}, \quad \lambda_1 = \frac{V(t)}{V(\tau)}.$$

In the steady-state case being considered here, the flow rate in the channel changes, and the velocity of the polymer solution is determined by the relation

$$V(x) = q/[D(x)W]. \tag{5}$$

Figure 2 compares the stresses $\tau_{xx} - \tau_{yy}$ calculated on the basis of Eqs. (3)-(5) with the stresses obtained on the axis of channels by the photoelastic method [see (1)]. On the whole, the agreement between the theoretical and experimental data is unsatisfactory, despite the rather broad assumptions made in the calculation. The greatest difference be-

tween the theoretical and experimental results is seen in the case of channels with curvature (Fig. 2d). The agreement here for channels with inlet angles $30 \leq 2\alpha \leq 90°$ indicates that the flow of a PABI solution in the plane-slit channels examined here is not accompanied by the formation of an inlet jet surrounded by recirculation zones.

Now let us examine flow in the channels of calibrated holes (model spinnerettes) and the expansion of the free jets at their outlets. The strain rates are considerably higher in this case than in the plane model channels and amount to $\sim 10^2$-10^4 sec^{-1}. Such values of strain rate are either on the order of τ_B^{-1} or exceed it (see the values of τ_B below), which means that in rheologically describing the flow, it is necessary to consider the tensility of the macromolecular subchains [7] and to use the RGE in the form (2) rather than reduced form (3).

Together with the above-cited values of G_0 and $\tau_1 = \tau_C$, in our calculations for the PABI solution we used the time $\tau_B = 5 \cdot 10^{-4}$ sec. Thus, $N = \tau_C/(3\tau_B) = 10$. Since the residence time of a fluid particle of the PABI solution in the convergent part of the channel of the model spinnerette $t_0 \sim 10^{-4}$-10^{-3} sec $\sim \tau_B$, we can drop the last term on the right from Eq. (2) and simplify the calculation of τ_2. The same applies to the calculations for the POD solution. For the latter, in accordance with the estimates in [1], we put $G_0 = 8 \cdot 10^3$ N/m^2, $\tau_C = 1.1$ sec, $\tau_B = 0.3$ sec, and $N = 1.22$ (the small difference in the concentration of the POD solutions examined here and in [1] was ignored; $t_0 < \tau_B$).

Examining the flow in the spinnerette channel as a flow associated with uniaxial tension, within the framework of the quasiunidimensional approximation we use Eqs. (2), (6)-(8), and (11) from [1] with allowance for the fact that, in the present case, the jet is free and the tractive force $F = 0$. Curves 1-4 in Figs. 3 and 4 show the results of calculations of values of the expansion coefficient of free jets at the outlet of the channels in the model spinnerettes B_*. Since, in accordance with [1], the value of τ_B for the POD solution is only approximate, we also performed calculations with $\tau_B = 0.03$ sec (dashed curves in Fig. 4).

It should be noted that in order to allow for the effect of purely viscous restructuring (relaxation) of the velocity profile in the jet, we followed [8, 9] and augmented the calculated value of the jet expansion coefficient by 0.1. Viscous relaxation of the velocity profile in the jet is a two-dimensional effect and is not considered in quasiunidimensional theory [1]. The relative contribution it makes to the jet expansion coefficient B_* is greater, the smaller the inlet angle α, i.e., the weaker the elongational effects compared to the shear effects.

On the other hand, the experimental data shown in Figs. 3 and 4 indicates that, in contrast to the case of plane-slit channels, with fairly large inlet angles ($2\alpha \gtrsim 25°$ for PABI and $2\alpha \gtrsim 40°$ for POD) an inlet jet surrounded by a stagnant zone is evidently formed in the conical part of the spinnerette channel. This leads to cessation of the increase in B_* with a further increase in α at fixed q. The formation of an inlet jet in the conical part of the spinnerette channel with sufficiently large inlet angles α is also a two-dimensional effect.

Comparison of the theoretical and experimental data in Figs. 3 and 4 makes it possible to distinguish an intermediate range of inlet angles in which two-dimensional effects (both shear effects and effects associated with the formation of an inlet jet) are minimal and the experimental values of B_* are satisfactorily predicted by quasiunidimensional theory [1]. Thus, the flow in spinnerette channels is mainly elongational in character in the range $20 \lesssim 2\alpha \lesssim 25°$ for a PABI solution and in the range $30 \lesssim 2\alpha \lesssim 40°$ for a POD solution.

It should be noted that longitudinal flow is considerably more effective than shear flow for stretching stiff-chain macromolecules [10]. Thus, the above ranges of spinnerette-channel inlet angles corresponding to elongational flow will be optimal for the formation of fibers from PABI and POD solutions.

To approximately account for the effect of the formation of an inlet jet in calculations of flows in spinnerette channels within the framework of the quasiunidimensional model [1] at angles $2\alpha \gtrsim 25°$ for PABI and $2\alpha \gtrsim 42°$ for POD, the values $2\alpha = 25°$ and $2\alpha = 42°$ should be taken for PABI and POD, respectively.

On the whole, comparison of the theoretical and experimental data in Figs. 3 and 4 shows that with reasonable semi-empirical accounting for two-dimensional effects, the quasi-unidimensional model [1] makes it possible to describe the expansion of free jets at the outlet of spinnerettes within a fairly broad range of flow rates for a polymer system.

NOTATION

λ, wavelength of monochromatic radiation; α, inlet angle of model plane channels or the channels of model spinnerettes; ℓ, length of channel; L_1 and L_2, lengths of the convergent part of the channel and the following part with a constant cross section; D, outlet width of the plane channel or outlet diameter of the spinnerette channel; D_0, inlet width or diameter of channel; W, width of the plane channel in the direction normal to the plane of the inset sketch in Fig. 2a; r, radius of curvature of the channel; η_0, viscosity at zero shear rate; $\overline{M}_W$, molecular weight; τ_{xy}, shear stress; N_1, first difference of the normal stresses in shear; $\dot{\gamma}$, shear rate; G and G_0, high-elasticity moduli; τ_{xx} and τ_{yy}, longitudinal and transverse components of the stress-tensor deviator τ; x, longitudinal coordinate, reckoned along the channel axis (y is reckoned normal to this axis) in the plane of the inset sketch in Fig. 2a; n, serial number of interference band; C, dynamic optical coefficient; d, thickness of the illuminated layer of the polymer solution; κ, extinction angle; ΔP, pressure gradient; q, rate of flow of polymer solution; B_*, jet expansion coefficient; D_+, diameter of jet after discharge from the spinnerette channel; $F_\tau(t)$, strain tensor-gradient from the past moment τ to the present moment t; Q, kinematic tensor in the Doi–Edwards RGE; I, unit tensor; u_0, unit vector randomly oriented in space; $\tau_1 = \tau_C$, maximum relaxation time in the Doi–Edwards RGE; t_0, characteristic residence time of fluid particle in convergent part of the channel; V, longitudinal velocity of polymer solution; D(x), width of the plane channel; τ_B, characteristic time of contraction (relaxation) of tensed subchains of a macromolecule; τ_2, stress tensor due to disequilibrium of the system of bonding points of the macromolecule; ∇v, velocity gradient tensor; D, strain-rate tensor; N, number of subchains in the macromolecule; F, tractive force in the jet.

LITERATURE CITED

1. T. M. Getmanyuk and A. L. Yarin, Inzh.-Fiz. Zh., 55, No. 1, 50-59 (1988).
2. A. Durelli and W. Riley, Introduction to Photomechanics [Russian translation], Moscow (1970).
3. G. E. Prozorova, A. V. Pavlov, V. N. Smirnova, et al., Vysokomol. Soedin., B20, No. 1, 48-51 (1978).
4. V. I. Brizitskii, A. I. Isaev, Yu. Ya. Podol'skii, et al., Inzh.-Fiz. Zh., 29, No. 6, 977-984 (1975).
5. G. A. Belinskii, V. I. Brizitskii, N. P. Kruchinin, et al., Khim. Volokna, No. 4, 25-28 (1982).
6. V. N. Tsvetkov, V. B. Novakovskii, N. A. Mikhailova, et al., Vysokomol. Soedin., A22, No. 1, 133-142 (1980).
7. A. L. Yarin, Dokl. Akad. Nauk SSSR, 292, No. 4, 854-858 (1987).
8. J. Gavis and M. Modan, Phys. Fluids, 10, No. 3, 487-497 (1967).
9. A. Ya. Malkin, V. V. Goncharenko, and V. V. Malinovskii, Mekh. Polim., No. 3, 487-492 (1976).
10. A. Chiferri and I. Ward, High-Molecular-Weight Polymers [Russian translation], Leningrad (1983).